THE JOURNAL OF PHYSICAL CHEMISTRY A

Article

Cite This: J. Phys. Chem. A 2019, 123, 5600−5612

pubs.acs.org/JPCA

Equilibrium Structures of the Phosphorus Trihalides PF_3 and PCl_3, and the Phosphoranes PH_3F_2, PF_5, PCl_3F_2, and PCl_5

Jürgen Breidung and Walter Thiel*

Max-Planck-Institut für Kohlenforschung, Kaiser-Wilhelm-Platz 1, D-45470 Mülheim an der Ruhr, Germany

Supporting Information

ABSTRACT: Among the title species, a reliable and accurate equilibrium geometry (r_e structure) is available only for PF_3, which has been determined experimentally more than 20 years ago. Here, we report accurate r_e structures for all title molecules, which were obtained using a composite computational approach based on explicitly correlated coupled-cluster theory (CCSD(T)-F12b) in conjunction with a large correlation-consistent basis set (cc-pCVQZ-F12) to take core−valence electron correlation into account. Additional terms were included to correct for the effects of iterative triple excitations (CCSDT), noniterative quadruple excitations (CCSDT(Q)), and scalar relativistic contributions (DKH2-CCSD(T)). The performance of this computational procedure was established through test calculations on selected small molecules (PH, PF, PCl, PH_2, PF_2, and PH_3). For PF_3, PCl_3, PH_3F_2, and PF_5 sufficiently accurate experimental ground-state rotational constants from the literature were used to determine semiexperimental r_e structures, which were found to be in excellent agreement with the corresponding best estimates from the current composite approach. The recommended equilibrium structural parameters are for PCl_3, $r_e(PCl)$ = 203.94 pm and $\theta_e(ClPCl)$ = 100.18°; for PH_3F_2, $r_e(PH_{eq})$ = 138.38 pm and $r_e(PF_{ax})$ = 164.15 pm; for PF_5, $r_e(PF_{eq})$ = 153.10 pm and $r_e(PF_{ax})$ = 157.14 pm; for PCl_3F_2, $r_e(PCl_{eq})$ = 200.21 pm and $r_e(PF_{ax})$ = 159.37 pm; and for PCl_5, $r_e(PCl_{eq})$ = 201.29 pm and $r_e(PCl_{ax})$ = 211.83 pm. The associated uncertainties are estimated to be ±0.10 pm and ±0.10°, respectively.

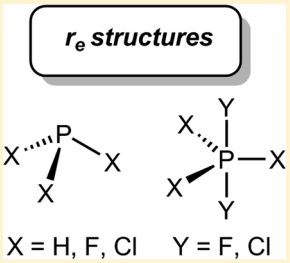

1. INTRODUCTION

The most meaningful representation of the geometry of a molecule is provided by its equilibrium structure (r_e structure), mainly because it is independent of vibrational effects. The advantage of such a vibrationless structure becomes obvious when comparing geometries of related molecules: even subtle effects that may have some influence on the structural parameters can be discussed in terms of differences in the chemical bonding in these species. Such a discussion is less straightforward when nuclear-motion effects must be taken into account. Of course, such comparisons are most meaningful when the r_e structures in question are as reliable and accurate as possible. At least they should have been determined in a consistent way, for instance by high-level quantum-chemical calculations. Sometimes it is feasible experimentally to correct the measured ground-state rotational constants of a given polyatomic molecule (and its isotopologues if necessary) for the contributions due to zero-point vibrations. The resulting equilibrium rotational constants may then be used to derive the equilibrium geometry. Among the title species, such a purely experimental procedure was applied to PF_3 (phosphorus trifluoride): the measured[1] constants B_0 and C_0 were converted[2] to the corresponding equilibrium values B_e and C_e to determine a reliable and accurate r_e structure of PF_3.[2] However, such a purely experimental procedure has not yet been applied to the other title molecules. For PCl_3 (phosphorus trichloride),[3−6] PH_3F_2 (difluorophosphorane),[7,8] and PF_5 (phosphorus pentafluoride)[9−12] ground-state rotational constants were measured, but there is not enough experimental information (vibration−rotation interaction constants) to transform them into equilibrium constants. For PCl_3F_2 (trichlorodifluorophosphorane) and PCl_5 (phosphorus pentachloride), spectroscopically derived rotational constants are not available at all.

Continuous advances in electronic structure methods and computational resources have made it possible to calculate the vibrational corrections to ground-state rotational constants of polyatomic molecules and their isotopologues with sufficient accuracy. Adopting these corrections, the resulting equilibrium rotational constants allow for the determination of the respective r_e structure, e.g., by a least-squares fitting procedure. Such a structure is called a semiexperimental equilibrium structure,[13] due to the combination of experimental and theoretical data. This strategy has been pioneered by the work of Pulay, Meyer, and Boggs about 40 years ago.[14] Its accuracy has been carefully established,[15] and it can nowadays be applied almost routinely (e.g., see ref 16).

Alternatively, equilibrium geometries of small and medium-sized molecules may also be obtained with an accuracy of about 0.1 pm for bond lengths and 0.1° for bond angles using state-of-the-art quantum-chemical methods. Typically, these methods are based on coupled-cluster (CC) theory including higher-order (at least quadruple) excitations and employing large basis sets, perhaps in combination with extrapolation

Received: May 9, 2019
Revised: June 7, 2019
Published: June 10, 2019

DOI: 10.1021/acs.jpca.9b04406
J. Phys. Chem. A 2019, 123, 5600−5612

techniques to estimate the complete basis set limit. Such rather expensive calculations have become feasible by the introduction of composite approaches.[17−20] Recently, we have reported[21] a composite procedure related to the so-called geometry scheme[20] whose dominant term is based on explicitly correlated CC theory (CCSD(T)-F12b)[22] and which takes core−valence electron correlation properly into account by employing an orbital basis set (cc-pCVQZ-F12) optimized for that purpose.[23] We have used this approach to calculate the equilibrium structural parameters of pyrazine (10 atoms), s-triazine (9 atoms), and s-tetrazine (8 atoms) with estimated uncertainties of ±0.10 pm and ±0.10° for bond distances and angles, respectively.[21] The largest species treated in that study[21] was benzene serving as a test molecule. We note that gradient schemes[18−20] have the advantage to provide stationary points corresponding to minima of the potential energy surface computed with a given approach. However, geometry schemes[20,21] are computationally less demanding[20] while they are capable of providing results that are very similar to those from gradient approaches.[20,21]

In the present paper we apply the composite computational approach of ref 21 to compute the equilibrium geometries of the title molecules. As already mentioned, a reliable and accurate r_e structure is available in the literature only for PF_3.[2] For PCl_3 and PF_5, r_e structures were estimated from corresponding zero-point average (r_z) structures.[25,26] Gas electron diffraction data measured[27] for PF_5 were reanalyzed[28] to deduce equilibrium values for the bond distances, which are identical to those from ref 26 within the quoted error bars. For PH_3F_2, the effective ground-state (r_0) structure was inferred from the associated ground-state rotational constants.[7,8] For PCl_3F_2, mean internuclear distances (r_g structure) were determined by gas-phase electron diffraction.[29] Finally, for PCl_5 average structural parameters denoted r_α, r_g, and r_a are available.[30,31]

Previously, we considered target and test molecules consisting only of first-row and hydrogen atoms.[21] We start our current investigation by demonstrating that the chosen computational procedure is capable of accurately describing also the geometries of selected test molecules containing second-row atoms (P and Cl), namely, PH ($X\ ^3\Sigma^-$), PF ($X\ ^3\Sigma^-$), PCl ($X\ ^3\Sigma^-$), PH_2 ($X\ ^2B_1$), PF_2 ($X\ ^2B_1$), and PH_3 ($X\ ^1A_1$). In addition, these small test species allow us to check convergence issues in our calculations. Unfortunately, the PCl_2 radical could not be included as a test species due to the lack of experimental data for rotational constants and equilibrium structural parameters. Whenever experimental ground-state rotational constants are known for the present target molecules, we determined a semiexperimental r_e structure to check the respective theoretical best estimate provided by the current purely computational scheme.

2. COMPUTATIONAL METHODS

We adopt the composite computational approach outlined in ref 21 to determine theoretical best estimates for the equilibrium bond length r_e and bond angle θ_e of each molecule, with a slight modification in the scalar relativistic part (see below). For the sake of easy reference and clarity, the basic definitions of this procedure[21] are repeated here (see eqs 1−4):

$$p_e(\text{best estimate}) = p_e[(\text{U})\text{CCSD(T)-F12b/CVQZ-F12}] + \Delta p_e[\text{T}] + \Delta p_e[(\text{Q})] + \Delta p_e[\text{SR}] \quad (1)$$

$$\Delta p_e[\text{T}] = p_e[(\text{ROHF-})\text{CCSDT/VTZ}] - p_e[(\text{ROHF-})\text{CCSD(T)/VTZ}] \quad (2)$$

$$\Delta p_e[(\text{Q})] = p_e[(\text{UHF-})\text{CCSDT(Q)/VDZ}] - p_e[(\text{UHF-})\text{CCSDT/VDZ}] \quad (3)$$

$$\Delta p_e[\text{SR}] = p_e[\text{DKH2-(U)CCSD(T)/AWCVTZ-DK}] - p_e[(\text{U})\text{CCSD(T)/AWCVTZ}] \quad (4)$$

As indicated by the first term on the right-hand side of eq 1, the structural parameter p_e (r_e or θ_e) is initially optimized at the level of explicitly correlated CC theory employing the so-called F12b approximation[22,32,33] including all single and double excitations (CCSD)[34,35] and augmented by a perturbational estimate of the effects of connected triple excitations (CCSD(T)).[36] CVQZ-F12 denotes the correlation-consistent polarized core−valence quadruple-ζ basis cc-pCVQZ-F12 optimized[23] for the explicitly correlated F12 methods.[22] At hydrogen, this basis reduces to the cc-pVQZ-F12 basis set.[24] The parameter p_e evaluated at the CCSD(T)-F12b/CVQZ-F12 level of theory is expected to be reasonably close to the basis set limit[22] and therefore serves as the starting point in the present scheme. For the purpose of comparison, we also tested the smaller basis CVTZ-F12, which is the correlation-consistent polarized core−valence triple-ζ basis cc-pCVTZ-F12[23] being equal to cc-pVTZ-F12[24] at hydrogen. For the open-shell species serving as test molecules (PH, PF, PCl, PH_2, and PF_2) the unrestricted UCCSD(T)-F12b variant[33,37] was used, which is based on a high-spin restricted open-shell Hartree−Fock (ROHF) determinant[38] and the perturbative triples corrections are computed as defined in ref 39. Whenever using core−valence basis sets in this work, all electrons in the molecule under consideration were correlated, except for those occupying the 1s-like core molecular orbitals (MOs) of the second-row atoms. All (U)CCSD(T)-F12b geometry optimizations were done using the MOLPRO 2012 program.[40,41] The four-point formula implemented in this program was used for the numerical energy gradients, and the step sizes for distances and angles were set to 0.01 a_0 and 0.5°, respectively. Throughout this work, the largest internal gradient components at the stationary points were always less than 2×10^{-6} E_h/a_0. For further technical details concerning the (U)CCSD(T)-F12b calculations, the reader is referred to ref 21.

The term $\Delta p_e[\text{T}]$ (see eqs 1 and 2) corrects the (U)CCSD(T)-F12b/CVQZ-F12 result for the effects of an iterative treatment of connected triple excitations. Accordingly, this term is obtained as the difference of p_e optimized at the level of CC theory with a full treatment of single, double, and triple excitations (CCSDT)[42,43] and at the CCSD(T)[34,36,44] level (see eq 2). The acronym VTZ refers to the correlation-consistent polarized valence triple-ζ basis cc-pVTZ[45] for the H and F atoms and the tight d-augmented cc-pV(T+d)Z[46] basis for the P and Cl atoms. To check basis set convergence in the case of the test molecules (PH, PF, PCl, PH_2, PF_2, and PH_3),

DOI: 10.1021/acs.jpca.9b04406
J. Phys. Chem. A 2019, 123, 5600−5612

Δp_e[T] was also calculated with the VQZ, V5Z, and up to V6Z basis sets, which are the n-tuple-ζ (n = 4, 5, 6) analogues[45−47] of VTZ (n = 3). Whenever such valence-only basis sets were used, the frozen core approximation was applied (i.e., the 1s2s2p-like core MOs of P and Cl and the 1s-like core MO of F were constrained to be doubly occupied). For the open-shell test molecules (see above) the ROHF-based variants of CCSDT[48] and CCSD(T)[39] were used. These geometry optimizations were performed using analytic or numerical energy gradients as implemented in the CFOUR program.[49]

The term Δp_e[(Q)] (see eqs 1 and 3) is computed as the difference of p_e optimized at the level of CCSDT augmented by a perturbative treatment of connected quadruple excitations (CCSDT(Q))[50,51] and at the CCSDT level. This approximate correction for the effects of quadruple excitations partly covers higher-order excitations in the cluster operator. The label VDZ stands for the double-ζ analogue of the VTZ basis.[45,46] To check basis set convergence in the case of the test molecules (see above), Δp_e[(Q)] was computed employing even larger basis sets (up to V6Z). The geometry optimizations at the CCSDT(Q) level were done with the use of the MRCC code[52,53] interfaced to CFOUR.[49] Numerical energy gradients as provided by CFOUR[49] had to be used for CCSDT(Q), whereas analytic[54] or numerical energy gradients were employed for CCSDT. For the test molecules, the CCSDT(Q) geometries were compared with those optimized at the level of CC theory with a full treatment of single, double, triple, and quadruple excitations (CCSDTQ),[53,55−57] employing basis sets up to VQZ. The CCSDTQ geometry optimizations were carried out in complete analogy to those at the CCSDT(Q) level. Due to program limitations, the CCSDT(Q) calculations had to be based on an unrestricted Hartree−Fock (UHF)[58] reference wave function for the open-shell test species. For the sake of compatibility, the corresponding CCSDTQ calculations were also carried out using a UHF reference function. Consequently, to be consistent within the Δp_e[(Q)] (and Δp_e[Q]) term the associated CCSDT calculations were also based on a UHF determinant (UHF-CCSDT)[48] in these cases.

The final term Δp_e[SR] (see eqs 1 and 4) serves as a correction for scalar relativistic effects on the given structural parameter p_e: This term was evaluated from the difference of p_e optimized at the CCSD(T) level using the Douglas−Kroll−Hess Hamiltonian of second order (DKH2)[59−61] and at the nonrelativistic (standard) CCSD(T) level. The acronym AWCVTZ refers to the augmented correlation-consistent polarized weighted core−valence triple-ζ basis (aug-cc-pwCVTZ).[62−64] To check basis set convergence, we employed the larger basis sets AWCVQZ and AWCV5Z, which are the quadruple-ζ and quintuple-ζ analogues[62−64] of AWCVTZ. At hydrogen, these basis sets reduce to the corresponding aug-cc-pVXZ (X = T, Q, 5) sets.[63] In conjunction with the DKH2 Hamiltonian, the correspondingly recontracted[65] versions of these basis sets were used (denoted as AWCVXZ-DK; X = T, Q, 5). We recall that the employment of a core−valence basis currently implies that all electrons in the molecule under study were correlated (see above for details). For the open-shell test species, these calculations were done using the unrestricted variant of CC theory based on ROHF orbitals (denoted UCCSD(T)).[39,66] The geometry optimizations concerning Δp_e[SR] were carried out using the MOLPRO 2012 program.[40] Numerical energy gradients were utilized in analogy to the (U)CCSD(T)-F12b calculations for the leading term in eq 1 (see above).

To summarize, the present composite approach was used to deduce theoretical best estimates of the geometry of the following molecules within the constraint of their point group symmetries:

1. Test molecules: diatomic radicals PH, PF, and PCl (X $^3\Sigma^-$; $C_{\infty v}$), triatomic radicals PH_2 and PF_2 (X $^2B_1$; C_{2v}), and PH_3 (C_{3v}).
2. Target molecules: PF_3 (C_{3v}), PCl_3 (C_{3v}), PH_3F_2 (D_{3h}), PF_5 (D_{3h}), PCl_3F_2 (D_{3h}), and PCl_5 (D_{3h}).

The experimental ground-state rotational constants of PH_2,[67] PD_2,[68] PF_2,[69] PH_3,[70] PD_3,[71] PF_3,[72] PCl_3,[5,6] PH_3F_2,[7,8] and PF_5[11,12] were used to determine a semiexperimental[13] r_e structure for these species. To be more specific, we utilized for the asymmetric top species PX_2 (X = H, D, F) the measured[67−69] constants A_0, B_0, and C_0, and for the oblate symmetric top molecules PH_3, PD_3, and PF_3 the B_0 and C_0 constants,[70−72] which refer to the so-called B-reduction of the rotational Hamiltonian for PH_3 and PD_3.[70,71] Furthermore, we used the B_0 constants[5,6] of the $P^{35}Cl_3$ and $P^{37}Cl_3$ isotopologues, as well as the published[7,8,11,12] A_0 and B_0 constants for the prolate symmetric tops PH_3F_2 and PF_5. In order to deduce the equilibrium rotational constants, the corresponding zero-point vibrational corrections[13,73,74] ΔX_{vib} (X = A, B, C) are needed. For this purpose, we determined the required cubic normal coordinate force constants at the (UHF-)CCSD(T) level of theory with the use of the CFOUR code,[49] employing various basis sets (see below) and using a finite difference procedure[75] that involved displacements along reduced (dimensionless) normal coordinates (step size Δq = 0.05) and the calculation of analytic Hessians[76,77] at these displaced geometries. At the respective equilibrium geometries optimized at the same level of theory as adopted for the force field calculations, the internal gradient components were always less than 2×10^{-10} E_h/a_0. The vibration−rotation interaction constants (α-constants) were derived from the theoretical normal coordinate force constants by applying standard formulas based on second-order rovibrational perturbation theory.[73] In addition, the α-constants of PCl_3F_2 and PCl_5 were also calculated. For PCl_5, only those parts of the cubic force field were computed that are required for the calculation of the α-constants[73] (using the CFOUR[49] input option ANHARMONIC = VIBROT). The following basis sets were employed: AVQZ for PH_2, PD_2, PF_2, PH_3, PD_3, PF_3,[72] $P^{35}Cl_3$, and $P^{37}Cl_3$; VQZ for PH_3F_2, PD_3F_2, PF_5, $P^{35}Cl_3F_2$, and $P^{37}Cl_3F_2$; VTZ for $P^{35}Cl_5$ and $P^{37}Cl_5$. The VQZ and VTZ basis sets have already been described (see above). The AVQZ basis is derived from VQZ by the addition of diffuse functions: it consists of the aug-cc-pVQZ[63] basis for H and F and aug-cc-pV(Q+d)Z[46] for P and Cl. Most of these results serve as predictions, in particular those for PD_3F_2, PCl_3F_2, and PCl_5 whose rotational constants have not yet been measured.

Besides the vibrational correction ΔX_{vib}, there is a small electronic (magnetic) contribution ΔX_{el}, which is related to the rotational g-tensor.[13,74,78] Such contributions were also included to investigate their effects on the semiexperimental structural parameters. Thus, the rotational g-tensors of the various species mentioned above were computed at the level of CCSD(T)/AWCVTZ theory at the associated best estimated equilibrium geometries from this study. The CFOUR[49] program was used for these computations to ensure gauge-origin independence and fast basis set convergence by employing rotational London atomic orbitals.[79,80] However,

DOI: 10.1021/acs.jpca.9b04406
J. Phys. Chem. A 2019, 123, 5600−5612

Table 1. Computed and Experimental Equilibrium Bond Lengths (pm) in PX (X = H, F, Cl)

		PH	PF	PCl
method[a]	basis	r_e(PH)[b]	r_e(PF)[b]	r_e(PCl)[b]
CCSD(T)	VDZ	143.78	164.16	205.53
CCSD(T)	VTZ	142.58	159.69	203.33
CCSD(T)	VQZ	142.40	159.41	202.38
CCSD(T)	V5Z	142.36	159.28	202.08
CCSD(T)	V6Z	142.35	159.22	201.95
CCSD(T)	AWCVTZ	142.23	159.59	202.88
CCSD(T)	AWCVQZ	142.11	159.10	201.74
CCSD(T)	AWCV5Z	142.07	158.89	201.46
DKH2-CCSD(T)	AWCVTZ-DK	142.24	159.65	202.93
DKH2-CCSD(T)	AWCVQZ-DK	142.12	159.16	201.79
DKH2-CCSD(T)	AWCV5Z-DK	142.09	158.95	201.51
CCSDT	VDZ	143.84[.84]	164.26[.26]	205.69[.68]
CCSDT	VTZ	142.63[.63]	159.76[.75]	203.47[.47]
CCSDT	VQZ	142.46[.46]	159.46[.46]	202.51[.51]
CCSDT	V5Z	142.41[.41]	159.32[.32]	202.20[.20]
CCSDT	V6Z	142.40[.40]	159.26[.26]	202.07[.07]
CCSDT(Q)	VDZ	143.85	164.35	205.75
CCSDT(Q)	VTZ	142.65	159.84	203.55
CCSDT(Q)	VQZ	142.47	159.54	202.59
CCSDT(Q)	V5Z	142.43	159.41	202.28
CCSDT(Q)	V6Z	142.42	c	c
CCSDTQ	VDZ	143.85	164.32	205.73
CCSDTQ	VTZ	142.65	159.81	203.54
CCSDTQ	VQZ	142.47	159.52	c
CCSD(T)-F12b	CVTZ-F12	142.09	158.87	201.39
CCSD(T)-F12b	CVQZ-F12	142.07	158.81	201.31
best estimate[a]		142.14	159.03	201.57
experimental[d]		142.182772(89)[e]	158.9329(20)	201.4609(49)
experimental[f]		142.2179(16)	158.96	
experimental[g]		142.140(22)		

[a]See text. [b]Decimal places in square brackets refer to the corresponding UHF-CCSDT results (see text). [c]Not calculated. [d]Reference 86 for PH, ref 89 for PF, and ref 91 for PCl. [e]Value determined for PD. [f]Reference 87 for PH and ref 90 for PF. [g]Reference 88.

due to program limitations the rotational g-tensors were not calculated for the open-shell molecules. All g-factors and ΔX_{el} values computed presently are contained in Tables S1 and S2 of the Supporting Information, together with the ΔX_{vib} data (see above). While most of the g-factors stand as predictions, they may be compared with experiment in a few cases, e.g., for PH_3[81] and PF_3.[82] It turned out that neglecting these electronic contributions has no significant impact on the present equilibrium geometrical parameters: the bond lengths and angles change at most by 0.0033 pm and 0.0026°, respectively (these maximum values apply to PCl_3), the only exception being r_e(PH) in PH_3F_2 where a somewhat larger effect (0.012 pm) occurs.

Several of the basis sets employed in calculations with the programs CFOUR[49] and MRCC[52] were downloaded from the EMSL basis set library using the Basis Set Exchange web portal.[83,84]

3. RESULTS AND DISCUSSION

3.1. Test Molecules. The computed equilibrium geometries of the diatomic test molecules PH, PF, and PCl are collected in Table 1, and those of PH_2, PF_2, and PH_3 are listed in Table 2. Considering the raw results, those calculated at the DKH2-(U)CCSD(T)/AWCV5Z-DK and (U)CCSD(T)-F12b/CVQZ-F12 levels of theory should be the most reliable and accurate ones, due to the size of the basis sets as well as the inclusion of core−valence electron correlation and scalar relativistic effects (in case of the DKH2 results). Moreover, structures optimized at the level of explicitly correlated CC theory are known to be reasonably close to the basis set limit.[22] For this reason, they were selected as starting points to derive theoretical best estimates for the r_e structures (see section 2).

Upon comparison of the results from (ROHF-)CCSDT/VTZ and (ROHF-)CCSD(T)/VTZ, the full treatment of connected triple excitations appears to increase the bond lengths in the test molecules, by +0.03 pm in PH_3 up to +0.14 pm in PCl. The bond angles in PH_2, PF_2, and PH_3 decrease very slightly (0.009−0.015°). Upon enlargement of the basis from VTZ to VXZ (X = 6 for PH, PF, PCl, and PH_2; X = 5 for PF_2 and PH_3), the effects arising from the full treatment of connected triple excitations change the bond distances in PH, PH_2, PF_2, and PH_3 minutely (at most by 0.01 pm), and only slightly more in PF and PCl (decreasing by 0.02−0.03 pm). The corresponding effect on the bond angle is negligible in PF_2 (by 0.001°) and still tiny in PH_2 and PH_3 (decrease in absolute value by 0.009° and 0.007°, respectively). Thus, typically, the CCSDT versus CCSD(T) corrections are already converged reasonably well for the VTZ basis. This is in line with previous observations.[17] Even in the two cases where the effects may not seem completely negligible (bond angles in PH_2 and PH_3), they are still so small in absolute value (on the order of 0.01°)

DOI: 10.1021/acs.jpca.9b04406
J. Phys. Chem. A 2019, 123, 5600−5612

Table 2. Computed and Semiexperimental Equilibrium Geometries (pm, deg) of PX_2 (X = H, F) and PH_3 as Well as Experimental Equilibrium Geometries (pm, deg) of PH_3

		PH_2		PF_2		PH_3	
method[a]	basis	r_e(PH)[b]	θ_e(HPH)[b]	r_e(PF)[b]	θ_e(FPF)[b]	r_e(PH)	θ_e(HPH)
CCSD(T)	VDZ	143.06	91.714	162.57	98.894	142.54	93.358
CCSD(T)	VTZ	141.99	91.840	158.39	98.657	141.56	93.505
CCSD(T)	VQZ	141.86	91.871	158.12	98.427	141.47	93.554
CCSD(T)	V5Z	141.83	91.878	157.96	98.350	141.44	93.560
CCSD(T)	V6Z	141.82	91.878	157.90	98.300	141.44	93.561
CCSD(T)	AWCVTZ	141.67	91.761	158.18	98.239	141.27	93.426
CCSD(T)	AWCVQZ	141.57	91.812	157.76	98.320	141.17	93.487
CCSD(T)	AWCV5Z	141.53	91.813	157.57	98.321	141.14	93.492
DKH2-CCSD(T)	AWCVTZ-DK	141.67	91.695	158.23	98.258	141.27	93.339
DKH2-CCSD(T)	AWCVQZ-DK	141.57	91.745	157.81	98.338	141.17	93.399
DKH2-CCSD(T)	AWCV5Z-DK	141.54	91.746	157.62	98.338	141.14	93.404
CCSDT	VDZ	143.11[.11]	91.695[.695]	162.66[.66]	98.887[.888]	142.57	93.344
CCSDT	VTZ	142.03[.03]	91.825[.825]	158.43[.43]	98.647[.649]	141.59	93.496
CCSDT	VQZ	141.90[.90]	91.862[.862]	158.15[.14]	98.417[.419]	141.50	93.550
CCSDT	V5Z	141.87[.87]	91.871[.871]	157.99[.99]	98.339[.341]	141.47	93.558
CCSDT	V6Z	141.86[.86]	91.872[.872]	c	c	c	c
CCSDT(Q)	VDZ	143.11	91.685	162.74	98.911	142.58	93.332
CCSDT(Q)	VTZ	142.04	91.806	158.50	98.669	141.60	93.474
CCSDT(Q)	VQZ	141.92	91.839	c	c	141.51	93.524
CCSDTQ	VDZ	143.11	91.684	162.72	98.908	142.58	93.331
CCSDTQ	VTZ	142.04	91.804	c	c	141.60	93.473
CCSD(T)-F12b	CVTZ-F12	141.55	91.747	157.55	98.291	141.15	93.454
CCSD(T)-F12b	CVQZ-F12	141.53	91.807	157.50	98.304	141.13	93.489
best estimate[a]		141.57	91.72	157.67	98.34	141.17	93.38
semiexperimental[a]		141.636(8)	91.686(13)	157.612(2)	98.338(2)	141.195	93.378
semiexperimental[a,d]		141.612(2)	91.706(3)			141.185	93.383
experimental[e]						141.1607(83)	93.4184(95)
experimental[e,f]						141.1785(57)	93.4252(68)

[a]See text. [b]Decimal places in square brackets refer to the corresponding UHF-CCSDT results (see text). [c]Not calculated. [d]Values evaluated for PD_2 and PD_3, respectively. [e]Reference 71. [f]Values determined for PD_3.

that they do not significantly affect the final theoretical best estimate of the associated r_e structures.

Higher-order correlation effects beyond CCSDT are approximated by the differences between (UHF-)CCSDT-(Q)/VDZ and (UHF-)CCSDT/VDZ results. Contributions from connected quadruple excitations to bond distances should converge faster with basis set size than those from connected triples.[17] In the current test molecules, the perturbative treatment of connected quadruples slightly increases the bond lengths. In the case of PH bonds (PH, PH_2, PH_3) the elongations do not exceed 0.01 pm. They are somewhat more pronounced for the PF and PCl bonds (0.07−0.09 pm). The bond angles in PH_2 and PH_3 decrease by 0.010° and 0.012°, respectively, whereas the angle in PF_2 increases by 0.023°. In the present test molecules, these contributions agree in sign with the corresponding (ROHF-)CCSDT versus (ROHF-)CCSD(T) differences (see above) so that both effects enhance each other. The only exception from this finding is provided by the bond angle in PF_2 for which a partial cancellation of both effects occurs. When enlarging the basis from VDZ to VXZ (X = 6 for PH; X = 5 for PF and PCl; X = Q for PH_2 and PH_3; X = T for PF_2), the effects of the connected quadruple excitations on the bond distances in the test molecules change typically at most by 0.01 pm. The effects on the bond angles in PH_2 and PH_3 are slightly larger (increase in absolute value by 0.013° and 0.014°, respectively) but remain small enough to not significantly affect the final theoretical best estimate of the associated r_e structures. In view of these data, we evaluate the (UHF-)CCSDT(Q) versus (UHF-)CCSDT contributions with the VDZ basis, assuming that they are sufficiently converged to serve as increments when deriving theoretical best estimates for the geometrical parameters, as in our previous study.[21] Generally, in order to achieve quantitative accuracy in the prediction of r_e structures quadruple excitations must be taken into account.[18,19] In this context, the question arises whether quadruple excitation effects on molecular geometries are sufficiently well described by the (UHF-)CCSDT(Q) approximation (i.e., by the noniterative treatment of quadruples). To check this issue, the geometries of the test molecules were additionally optimized at the (UHF-)CCSDTQ/VDZ level of theory. We find that the bond lengths in PH, PH_2, and PH_3 remain unaltered upon a full rather than a perturbative treatment of quadruple excitations. The bond distances in PF, PCl, and PF_2 are shortened by 0.02−0.03 pm. The bond angles in PH_2, PF_2, and PH_3 decrease by 0.001−0.003°. Essentially the same alterations occur in those cases where larger basis sets (VTZ, VQZ) could be employed (see Tables 1 and 2). Keeping in mind that the target accuracy of the present study is ±0.10 pm for bond lengths and ±0.10° for bond angles, these deviations are considered small enough to justify the use of the noniterative (UHF-)CCSDT(Q) approximation.

Scalar relativistic effects on the equilibrium molecular geometries are presently evaluated from the differences

DOI: 10.1021/acs.jpca.9b04406
J. Phys. Chem. A 2019, 123, 5600−5612

Table 3. Computed, Semiexperimental, and Experimental Equilibrium Geometries (pm, deg) of PF_3 and PCl_3

		PF_3		PCl_3	
method	basis	r_e(PF)	θ_e(FPF)	r_e(PCl)	θ_e(ClPCl)
CCSD(T)	VDZ	160.84[a]	97.500[a]	207.32	100.517
CCSD(T)	VTZ	156.84[a]	97.662[a]	205.64	100.384
CCSD(T)	VQZ	156.61[a]	97.593[a]	204.74	100.249
CCSD(T)	AVQZ	156.71[a]	97.525[a]	204.79	100.171
CCSD(T)	AWCVTZ	156.61	97.494	205.16	100.189
CCSD(T)	AWCVQZ	156.24[a]	97.565[a]	204.14	100.198
DKH2-CCSD(T)	AWCVTZ-DK	156.65	97.496	205.21	100.186
DKH2-CCSD(T)	AWCVQZ-DK	156.28[a]	97.566[a]	204.19	100.194
CCSDT	VDZ	160.90[a]	97.492[a]	207.43	100.526
CCSDT	VTZ	156.86[a]	97.656[a]	205.72	100.397
CCSDT	VQZ	156.62	97.589	*b*	*b*
CCSDT(Q)	VDZ	160.98[a]	97.503[a]	207.50	100.533
CCSDT(Q)	VTZ	156.93	97.665	*b*	*b*
CCSD(T)-F12b	CVTZ-F12	156.05	97.556	203.80	100.191
CCSD(T)-F12b	CVQZ-F12	156.00[a]	97.556[a]	203.75	100.171
best estimate[c]		156.14[d]	97.56[d]	203.95	100.19
semiexperimental[c]		156.10(10)	97.57(10)	203.94(10)	100.18(10)
experimental[e]		156.099(14)	97.57(4)	203.9(3)	100.28(10)[f]
experimental[g]		156.1(1)	97.7(2)		

[a]From ref 72. [b]Not calculated. [c]See text. [d]Numerically identical to the best estimate in ref 72. [e]Reference2 for PF_3 and ref 25 for PCl_3. [f]Estimate of uncertainty from ref 95. [g]Reference 94.

between the DKH2-(U)CCSD(T)/AWCVTZ-DK and (U)-CCSD(T)/AWCVTZ results. On an absolute scale, these effects are quite small for molecules containing first- and second-row atoms only:[85] the bonds in PF, PF_2, and PCl are lengthened by 0.05−0.06 pm, whereas the bond distances in PH, PH_2, and PH_3 remain virtually unchanged. The bond angles in PH_2 and PH_3 decrease by 0.066° and 0.087°, respectively, whereas the angle in PF_2 increases by 0.019°. To examine basis set convergence, we performed analogous geometry optimizations at the (U)CCSD(T) level of theory with and without the DKH2 Hamiltonian employing the AWCVQZ and AWCV5Z basis sets. The DKH2 calculations were carried out using the corresponding recontracted[65] basis sets, as before (see Tables 1 and 2). It turns out that the scalar relativistic effects calculated with the AWCVTZ basis vary in absolute value at most by 0.01 pm and 0.002°, respectively, when enlarging the basis as stated above. Thus, basis set convergence of the scalar relativistic effects appears to be reached for the AWCVTZ basis.

Tables 1 and 2 also show the best estimates of the r_e structures of the test molecules resulting from the current composite approach. They may be compared with the corresponding experimental r_e structures for PH,[86−88] PF,[89,90] PCl,[91] and PH_3.[71] However, for PH_2 and PF_2 there are no such experimental data available in the literature. For this reason semiexperimental r_e structures were determined for the PX_2 (X = H, D, F) species (see section 2). These structural data and their uncertainties were evaluated from the semiexperimental rotational constants A_e, B_e, and C_e in complete analogy to the procedure used to infer the experimental r_0 structure of PF_2.[69] Using the experimental[67−69] ground-state rotational constants, the corresponding inertial defects Δ_0 are presently calculated to be 0.0688 (PH_2), 0.0958 (PD_2), and 0.1906 u Å^2 (PF_2) whereas the respective semiexperimental equilibrium values Δ_e appear to be −0.000861, −0.000443, and +0.00202 u Å^2. As expected, the Δ_e values are significantly closer to zero than their Δ_0 counterparts. Additionally, we have determined semiexperimental r_e structures for PH_3 and PD_3 (see section 2), the uncertainties of which should be roughly similar to those from experiment.[71] We note that the calculated electronic contributions to the rotational constants (see Table S2 of the Supporting Information) have a particularly small effect on the semiexperimental r_e structures of PH_3 and PD_3: in the former, the bonds are lengthened by 0.00017 pm and θ_e(HPH) decreases by 0.0013° due to the magnetic corrections, while in the latter the corresponding effects are smaller by about a factor of 2 (0.000081 pm and 0.00063°, respectively). Thus, the neglect of these corrections in the experimental[71] determination of the r_e structures of PH_3 and PD_3 is fully justified by these results. The semiexperimental r_e structures of both species are in excellent agreement with their purely experimental[71] counterparts (see Table 2).

The deviations between the best estimated bond lengths and their experimental or semiexperimental analogues usually do not exceed 0.10 pm. A slightly larger deviation (0.11 pm) occurs for the internuclear distance in the PCl radical. The best estimated bond angles in PH_2, PF_2, and PH_3 agree with the semiexperimental and experimental[71] values, respectively, to within 0.05° (see Table 2). Applying a similar computational scheme as adopted presently, the r_e structure of PH_2 was best estimated[92] to be r_e(PH) = 141.58 pm and θ_e(HPH) = 91.78°. Scalar relativistic effects on the molecular geometry were neglected.[92] The corresponding correction indeed vanishes for the bond distance in PH_2 whereas relativity appears to narrow the bond angle by 0.066° (see Table 2). When excluding this correction, our current best estimate for the PH_2 structure is r_e(PH) = 141.57 pm and θ_e(HPH) = 91.78°, which is in almost perfect agreement with the result from ref 92 (see above).

In our previous investigation,[21] we noted that structural data computed at the CCSD(T)-F12b/CVQZ-F12 level of theory differ from those obtained at the CCSD(T)-F12b/CVTZ-F12 level at most by 0.02 pm and 0.04°, respectively. However, this

DOI: 10.1021/acs.jpca.9b04406
J. Phys. Chem. A 2019, 123, 5600−5612

Table 4. Computed and Semiexperimental Equilibrium as Well as Experimental Effective Ground-State Structures (pm) of PH_3F_2 and PF_5 and Experimental Equilibrium and Mean Internuclear Distances (pm) in PF_5

		PH_3F_2		PF_5	
method	basis	$r_e(PH_{eq})$[a]	$r_e(PF_{ax})$[a]	$r_e(PF_{eq})$[a]	$r_e(PF_{ax})$[a]
CCSD(T)	VDZ	139.89	167.02	157.29	160.82
CCSD(T)	VTZ	138.82	164.14	153.89	157.73
CCSD(T)	VQZ	138.78	164.33	153.68	157.64
CCSD(T)	AVQZ	138.80	164.72	153.74	157.72
CCSD(T)	AWCVTZ	138.49	164.68	153.57	157.64
CCSD(T)	AWCVQZ	138.46	164.27	153.25	157.32
DKH2-CCSD(T)	AWCVTZ-DK	138.43	164.73	153.56	157.64
DKH2-CCSD(T)	AWCVQZ-DK	138.40	164.32	153.24	157.31
CCSDT	VDZ	139.92	167.06	157.33	160.86
CCSDT	VTZ	138.84	164.16	153.90	157.74
CCSDT(Q)	VDZ	139.93	167.11	157.40	160.92
CCSD(T)-F12b	CVTZ-F12	138.46	164.03	153.10	157.12
CCSD(T)-F12b	CVQZ-F12	138.45	164.00	153.06	157.08
best estimate[b]		138.42	164.12	153.13	157.15
semiexperimental[b]		138.38(10)	164.15(10)	153.10(10)	157.14(10)
experimental[c]				152.9(3)	157.6(3)
experimental[d]				153.0	157.6
r_0 structure[e]		139.4(2)	164.68(2)	153.43(30)[f]	157.46(30)[f]
r_g structure[g]				153.4(4)	157.7(5)

[a]Subscripts eq and ax refer to equatorial and axial ligands, respectively. [b]See text. [c]Reference 26. [d]Reference 28. [e]References 7 and 8 for PH_3F_2 and ref 12 for PF_5. [f]Estimate of uncertainties from ref 95. [g]Reference 27.

observation[21] refers to molecules consisting only of first-row atoms and hydrogen. Considering the test molecules of this paper, the deviations may be somewhat larger: 0.02−0.08 pm and 0.01−0.06°, respectively. Similar deviations are seen for the title molecules (see below), with the notable exception of the axial bond length in PCl_5 (0.13 pm). Thus, in the presence of second-row atoms the significantly smaller CVTZ-F12 basis may be employed for the calculation of molecular geometries whenever the larger basis set is no longer feasible due to the size of the molecule under study or when the target accuracy is somewhat relaxed.

The results obtained for the best estimated r_e structures of the test molecules suggest that the current composite approach is suited to predict equilibrium bond lengths and angles with an accuracy of about ±0.10 pm and ±0.10°, respectively, even if second-row atoms are present. Therefore, the same accuracy is expected to be achievable for the actual target molecules (see also ref 93).

3.2. PF_3 and PCl_3. Table 3 collects the computed equilibrium structural parameters of PF_3 and PCl_3 which are needed in the present composite approach to derive the theoretical best estimates of the corresponding r_e structures. The latter are also given in Table 3. We include some further theoretical results, which are not involved in the evaluation of the best estimates but may be useful to check convergence issues. We point out that many results concerning PF_3 have already been published previously[72] (see Table 3, footnote *a*) and are included in Table 3 for the sake of easy reference. They are discussed in more detail in ref 72.

The current semiexperimental r_e structure of PF_3 is identical with its experimental[2] counterpart (see Table 3), both with regard to the estimated uncertainties of the former (±0.10 pm and ±0.10°, respectively) and the even smaller experimental[2] error bars (±0.014 pm and ±0.04°, respectively). The best estimated r_e structure is also in excellent agreement with experiment[2] (see Table 3). For the sake of completeness, Table 3 also contains another experimental equilibrium geometry of PF_3 determined in an earlier investigation.[94] Both experimental[2,94] r_e structures are in complete accordance when considering the uncertainties (±0.1 pm and ±0.2°, respectively) quoted in ref 94. In view of the agreement with the current theoretical best estimate and the semiexperimental result, the purely experimental[2] r_e structure appears to be the most reliable and accurate equilibrium geometry of PF_3 presently available. Thus, it is the recommended r_e structure for PF_3 (see Table 3).

Turning to PCl_3, the current semiexperimental r_e structure is almost identical with the theoretical best estimate, the differences (0.01 pm and 0.01°, respectively) being 1 order of magnitude smaller than the expected uncertainties (±0.10 pm and ±0.10°, respectively) of both of them. This excellent agreement validates both results. The molecular structure of PCl_3 was investigated by gas electron diffraction;[96] this study provided an r_a structure at two different temperatures, an estimate of the differences $r_a - r_e$, and hence a first estimate of the equilibrium geometry of PCl_3. The most reliable r_e structure of PCl_3 published[25] so far was derived from the r_z structure; it is identical with the semiexperimental r_e structure, within the corresponding uncertainties (see Table 3). However, we expect the present semiexperimental structural parameters to be superior in terms of reliability and accuracy, and we thus recommend the following equilibrium geometry for PCl_3: $r_e(PCl)$ = 203.94(10) pm and $\theta_e(ClPCl)$ = 100.18(10)°. The additional inclusion of the ground-state rotational constants[5] of the $P^{35}Cl_2{}^{37}Cl$ species through an unweighted least-squares structural fit (using the STRFIT code of Kisiel[97]) after having corrected them for the effects of zero-point vibrations and electronic contributions (see Table S1 of the Supporting Information) does not alter the recommended geometry significantly: $r_e(PCl)$ decreases by 0.01 pm and $\theta_e(ClPCl)$ increases by 0.01°. These changes are 1 order of

DOI: 10.1021/acs.jpca.9b04406
J. Phys. Chem. A 2019, 123, 5600−5612

magnitude smaller than the estimated error limits and are therefore currently neglected.

In contrast to PF_3 whose ground-state rotational constants are well determined experimentally (see refs 1 and 72 as well as references therein), the axial ground-state rotational constants C_0 of $P^{35}Cl_3$ and $P^{37}Cl_3$ have not yet been measured. Making use of the theoretical best estimate of the r_e structure, the rotational constants of $P^{35}Cl_3$ ($P^{37}Cl_3$) are calculated to be B_e = 2623.81 (2493.77) MHz and C_e = 1476.09 (1396.35) MHz (same unit as in the experimental work[3−6]). Adopting theoretical (CCSD(T)/AVQZ) vibrational and theoretical (CCSD(T)/AWCVTZ) electronic corrections, the ground-state rotational constants amount to B_0 = 2616.83 (2487.24) MHz and C_0 = 1470.38 (1391.04) MHz. Analogously, we obtain for $P^{35}Cl_2{}^{37}Cl$: A_0 = 2615.64 MHz, B_0 = 2531.29 MHz, and C_0 = 1443.32 MHz. It comes as no surprise that the electronic contributions are smaller in absolute value than the corresponding vibrational corrections (see Table S1 of the Supporting Information). The experimental[5,6] B_0 values of $P^{35}Cl_3$ and $P^{37}Cl_3$ as well as the experimental[5] X_0 (X = A, B, C) constants of $P^{35}Cl_2{}^{37}Cl$ are underestimated theoretically by 0.02%. The errors of the C_0 values predicted for the two totally symmetric species of PCl_3 are expected to be very similar to those of the other constants. Using the r_0 structure of PCl_3 from ref 5 C_0 is tentatively estimated to be 1474 (1394) MHz, thus being about 0.2% larger than our best C_0 values predicted above for $P^{35}Cl_3$ ($P^{37}Cl_3$).

3.3. PH_3F_2 and PF_5. Table 4 contains the calculated bond lengths in PH_3F_2 and PF_5, in particular those needed to arrive at the theoretical best estimates of the r_e structures. Both molecules assume a trigonal bipyramidal geometry.[7,27] According to Muetterties' rule,[98,99] the two axial positions will be occupied by the most electronegative ligands. The structure of PH_3F_2 conforms to this rule, i.e., the H (F) atoms take up the equatorial (axial) sites resulting in D_{3h} point-group symmetry, just as in PF_5. PH_3F_2 and PF_5 are examples of hypervalent species. Although a discussion of hypervalency[100] is beyond the scope of this paper, we note that a decade ago a new model of hypervalent bonding has been introduced[101] termed recoupled pair bonding. This concept has also been applied to the series of PF_n (n = 1−5) species.[102]

Turning to the equilibrium geometry of PH_3F_2, the best estimated r_e structure and its semiexperimental counterpart are in excellent agreement, with deviations of only 0.04 and 0.03 pm for $r_e(PH_{eq})$ and $r_e(PF_{ax})$, respectively (see Table 4). As before, the error bars of the semiexperimental r_e distances are assumed to equal those typically observed for the best estimates in our test calculations (±0.10 pm; see subsection 3.1). Experimentally,[7,8] only the effective ground-state structure of PH_3F_2 is available. As expected, the semiexperimental and the best estimated PH and PF equilibrium bond lengths are smaller than the associated r_0 distances, by about 1.0 and 0.5 pm, respectively (see Table 4).

The theoretical best estimate for the r_e structure implies the following values for the rotational constants of PH_3F_2 (PD_3F_2): A_e = 2.909996 (1.456117) cm^{-1} and B_e = 0.160179 (0.155895) cm^{-1} (same unit as in the experimental work[7,8]). Applying both theoretical (CCSD(T)/VQZ) vibrational and theoretical (CCSD(T)/AWCVTZ) electronic corrections, we obtain A_0 = 2.866446 (1.440804) cm^{-1} and B_0 = 0.159112 (0.154924) cm^{-1}. Compared to experiment,[7,8] the purely theoretical A_0 and B_0 constants of PH_3F_2 are too low by 0.054% and too large by 0.031%, respectively. In this context we note that the uncertainty of the experimental[7,8] A_0 value was estimated[8] to be 0.003 cm^{-1}, which corresponds to 0.105%, about twice as much as the error of the theoretical A_0 value. The rotational constants given above for PD_3F_2 serve as predictions. The associated errors should be about the same as those in PH_3F_2.

Turning to PF_5, the situation is very similar to that found for PH_3F_2 as well as for PF_3 and PCl_3: the best estimated and the semiexperimental r_e structures are essentially the same, the deviations being as small as 0.03 and 0.01 pm, respectively, for the equatorial and axial bond distances (see Table 4). The most recent experimental[26] r_e structure of PF_5 was derived from the r_z structure. Prior to this experimental work,[26] the gas electron diffraction data[27] were reanalyzed[28] to deduce not only a barrier height (3.4 kcal/mol) for the pseudorotation[103] in PF_5 but also the equilibrium internuclear distances (see Table 4, no uncertainties quoted in ref 28). The two experimental[26,28] r_e structures agree within the error limits of ±0.3 pm estimated in the more recent work.[26] Comparing the semiexperimental r_e structure with experiment,[26] the equatorial bond lengths differ by 0.2 pm, which is still covered by the experimental[26] uncertainty, whereas the difference between the axial bond lengths is somewhat more pronounced (0.46 pm). Similar to PH_3F_2, there is also an experimental[12] r_0 structure for PF_5 which was determined from the measured[11,12] A_0 and B_0 constants. As expected, the r_0 bond lengths are somewhat larger (by about 0.3 pm) than their semiexperimental r_e counterparts (see Table 4). While the equatorial r_0 bond lengths are also larger (0.4−0.5 pm) than their experimental[26,28] r_e analogues, in contrast to expectation this does not hold for the axial bonds. However, a definitive assessment is difficult due to the relatively large uncertainties (±0.3 pm)[26,95] of these structures.[12,26]

The equatorial r_e distance in PF_5 is shorter than the equilibrium bond length in PF_3 by about 3 pm (see Tables 3 and 4 for the best estimated, semiexperimental, and experimental r_e structures). Similarly, the PH r_e distance in PH_3F_2 is shorter than the equilibrium bond length in PH_3 by about 2.8 pm (see Tables 2 and 4). The axial r_e distance in PF_5 turns out to be much smaller than in PH_3F_2, by about 7 pm (see Table 4). It is well-known that the axial bonds in PF_5 are distinctly longer than the equatorial ones.[27] Considering the best estimated and semiexperimental r_e as well as the r_0 structure,[12] this difference appears to be 4.0 pm, in good agreement with the result from gas electron diffraction.[27]

Using the theoretical best estimate of the r_e structure, the rotational constants of PF_5 are calculated to be A_e = 3781.45 MHz and B_e = 3145.63 MHz (same unit as in the experimental work[11,12]). With the use of theoretical (CCSD(T)/VQZ) vibrational and theoretical (CCSD(T)/AWCVTZ) magnetic corrections we obtain A_0 = 3765.39 MHz and B_0 = 3132.61 MHz. The experimental[11,12] values for A_0 and B_0 in PF_5 are underestimated theoretically by 0.025−0.035%.

We complete this discussion for PH_3F_2 and PF_5 by emphasizing that the semiexperimental r_e structures of both species are in excellent agreement with the corresponding theoretical best estimates. Thus, both types of results validate each other. Therefore, we recommend the semiexperimental r_e structures of PH_3F_2 and PF_5 (see Table 4) as the most reliable and accurate equilibrium geometries available at present for these two species.

3.4. PCl_3F_2 and PCl_5. The computed equilibrium bond lengths including the best estimates for PCl_3F_2 and PCl_5 are

DOI: 10.1021/acs.jpca.9b04406
J. Phys. Chem. A 2019, 123, 5600−5612

Table 5. Computed Equilibrium and Experimental Average Structural Parameters (pm) of PCl_3F_2 and PCl_5

		PCl_3F_2		PCl_5	
method	basis	$r_e(PCl_{eq})$[a]	$r_e(PF_{ax})$[a]	$r_e(PCl_{eq})$[a]	$r_e(PCl_{ax})$[a]
CCSD(T)	VDZ	202.85	163.57	204.97	214.94
CCSD(T)	VTZ	202.02	159.73	203.14	213.22
CCSD(T)	VQZ	201.11	159.74	202.14	212.59
CCSD(T)	AVQZ	201.06	159.95	202.14	212.73
CCSD(T)	AWCVTZ	201.23	159.84	202.40	213.03
CCSD(T)	AWCVQZ	200.42	159.52	201.46	212.08
DKH2-CCSD(T)	AWCVTZ-DK	201.22	159.89	202.43	213.03
DKH2-CCSD(T)	AWCVQZ-DK	200.40	159.56	201.49	212.08
CCSDT	VDZ	202.93	163.62	205.08	215.04
CCSDT	VTZ	202.07	159.75	203.21	213.30
CCSDT(Q)	VDZ	203.00	163.68	205.17	215.09
CCSD(T)-F12b	CVTZ-F12	200.11	159.31	201.14	211.83
CCSD(T)-F12b	CVQZ-F12	200.10	159.24	201.10	211.70
best estimate[b]		200.21	159.37	201.29	211.83
r_g structure[c]		200.5(3)	159.6(2)	202.3(3)	212.7(3)
r_α structure[d]				201.7(3)	212.4(3)

[a]Subscripts eq and ax refer to equatorial and axial ligands, respectively. [b]See text. [c]Reference 29 for PCl_3F_2 and ref 30 for PCl_5. [d]Reference 30.

reported in Table 5. The rotational constants of both species have not yet been measured. Therefore, the semiexperimental strategy[13] could not be applied in these two cases. However, the r_g structures of both phosphoranes as well as the r_α and r_a structures of PCl_5 are known from gas electron diffraction studies.[29−31] The experimental[29,30] r_g and r_α internuclear distances are listed in Table 5. Like PH_3F_2 and PF_5 (see subsection 3.3), PCl_3F_2 and PCl_5 form trigonal bipyramidal molecules of D_{3h} point-group symmetry in the gas phase.[29−31] Appropriate to Muetterties' rule,[98,99] in PCl_3F_2 the most electronegative ligands (F atoms) occupy the two axial positions such that the equatorial sites are left over for the less electronegative ligands (Cl atoms).

As suggested by our current test calculations and by the results obtained for PF_3, PCl_3, PH_3F_2, and PF_5 (see above), the best estimated bond lengths in PCl_3F_2 and PCl_5 are expected to be accurate to within ±0.10 pm. In the absence of any semiexperimental or experimental equilibrium geometries for these two species, it is obvious that our best estimates are the most reliable and accurate r_e structures available to date for PCl_3F_2 and PCl_5 (see Table 5).

In PCl_3F_2, the best estimated PCl and PF r_e distances are smaller than the corresponding r_g values[29] by 0.3 and 0.2 pm, respectively. Qualitatively, this is in line with expectation. However, we note that these differences are still covered by the experimental[29] error limits (see Table 5). The PCl bonds in PCl_3F_2 may be compared with those in PCl_3, showing that the best estimated PCl r_e distance is smaller in the phosphorane species by 3.7 pm (see Tables 3 and 5). The comparison of the axial bonds in PCl_3F_2 with those in PF_5 reveals that substitution of the equatorial F by Cl atoms elongates these bonds by 2.2 pm (best estimate; see Tables 4 and 5). In the corresponding r_g structures,[27,29] this elongation is slightly smaller (1.9 pm).

Using the theoretical best estimate of the r_e structure of PCl_3F_2, the rotational constants of $P^{35}Cl_3F_2$ ($P^{37}Cl_3F_2$) are calculated to be B_e = 1647.47 (1585.41) MHz and C_e = 1201.83 (1136.90) MHz. Taking into account theoretical (CCSD(T)/VQZ) vibrational and theoretical (CCSD(T)/AWCVTZ) electronic corrections yields B_0 = 1642.23 (1580.47) MHz and C_0 = 1197.92 (1133.27) MHz. On the basis of our experience with analogously computed rotational constants of PF_3 (see ref 72), PCl_3 (see subsection 3.2), PH_3F_2 and PF_5 (see subsection 3.3), the B_0 and C_0 values predicted for PCl_3F_2 should be accurate to within 0.05%.

In PCl_5, the bond lengths at equilibrium (best estimates) are distinctly shorter than the corresponding r_g distances,[30] by 1.0 and 0.9 pm, respectively, for the equatorial and axial bonds. These differences correspond to at least three times the experimental[30] uncertainties (see Table 5), which appears to be quite substantial. This is in contrast to the situation in PCl_3F_2 (see above). The associated $r_\alpha - r_e$ differences are somewhat less pronounced (0.4 and 0.6 pm, respectively). The axial bonds in PCl_5 are much longer than the equatorial ones, according to the best estimates by 10.5 pm. Similar such differences are found in the r_g (10.4(4) pm) and r_α (10.7(4) pm) structures.[30] In PF_5, the corresponding difference is considerably smaller (close to 4 pm; see above). Replacing the axial F atoms in PCl_3F_2 by Cl atoms lengthens the equatorial PCl bonds by 1.1 pm (best estimate). This effect seems to be more pronounced (1.8(4) pm) when the equatorial r_g distances in PCl_5 are compared with those in PCl_3F_2 (see Table 5).

The best estimated r_e structure of PCl_5 implies that the rotational constants of $P^{35}Cl_5$ ($P^{37}Cl_5$) are A_e = 1188.97 (1124.74) MHz and B_e = 960.15 (908.28) MHz. Correcting them for the effects of zero-point nuclear motions (CCSD(T)/VTZ) and for electronic contributions (CCSD(T)/AWCVTZ) results in A_0 = 1184.94 (1120.99) MHz and B_0 = 956.82 (905.18) MHz. Just as for PCl_3F_2, the values of the rotational constants of PCl_5 serve as predictions whose maximum errors should not exceed 0.05% (see above).

4. CONCLUSIONS

Accurate molecular equilibrium geometries of selected trivalent (PF_3 and PCl_3) and pentavalent (PH_3F_2, PF_5, PCl_3F_2, and PCl_5) phosphorus compounds are reported. These geometries were calculated by means of a composite *ab initio* approach, which is based on explicitly correlated coupled-cluster theory (CCSD(T)-F12b) employing a large correlation-consistent orbital basis set (CVQZ-F12) to include core−valence electron correlation. The equilibrium structures optimized at this level

DOI: 10.1021/acs.jpca.9b04406
J. Phys. Chem. A 2019, 123, 5600−5612

of theory are corrected for the effects of an iterative treatment of triple excitations (CCSDT/VTZ versus CCSD(T)/VTZ) and of a noniterative treatment of quadruple excitations (CCSDT(Q)/VDZ versus CCSDT/VDZ). Scalar relativistic effects (DKH2-CCSD(T)/AWCVTZ-DK versus CCSD(T)/AWCVTZ) are also included.

Extensive test calculations on diatomic (PH, PF, PCl) and triatomic (PH_2, PF_2) radicals as well as on phosphane (PH_3) establish the accuracy of the composite procedure. The errors of the best estimated bond lengths usually do not exceed ±0.10 pm, and the best estimated bond angles turn out to be accurate to within ±0.05°. We find that basis set convergence of the leading term of the composite approach is not as fast as observed previously in molecules consisting only of first-row atoms and hydrogen.[21] Generally speaking, the CVQZ-F12 basis may often be replaced by the smaller CVTZ-F12 basis without significant loss of accuracy, but doing so seems to compromise the present target accuracy of ±0.10 pm in some cases, for example in the case of the axial bond lengths in PCl_5 (see Table 5).

For PF_3, PCl_3, PH_3F_2, and PF_5 sufficiently accurate ground-state rotational constants are available from high-resolution rotational and vibrational spectroscopy. We corrected these constants for the effects of zero-point vibrations (CCSD(T)/AVQZ and CCSD(T)/VQZ, respectively) and for electronic contributions related to the rotational g-tensor (CCSD(T)/AWCVTZ). The resulting empirical equilibrium rotational constants were used to determine semiexperimental r_e structures of these molecules. Throughout we find that these structures are in excellent agreement with the corresponding best theoretical estimates. This cross-validation confirms the accuracy of both approaches and suggests that best theoretical estimates can be used confidently instead of the semi-experimental r_e structures for species whose rotational constants have not yet been measured. The magnetic corrections of the experimental ground-state rotational constants are generally found to be negligible for structural purposes. In the case of PCl_3, PH_3F_2, and PF_5 we recommend the current semiexperimental r_e structures (essentially identical with the best estimates; see Tables 3 and 4), whereas for PF_3 the purely experimental[2] r_e structure continues to be the most reliable and accurate equilibrium geometry published to date.

The best estimated equilibrium geometries of PCl_3F_2 and PCl_5 are expected to be of the same accuracy (±0.10 pm for bond lengths) as those for PF_3, PCl_3, PH_3F_2, and PF_5. Therefore, we recommend these best estimates as the most reliable and accurate r_e structures of PCl_3F_2 and PCl_5 available at present (see Table 5).

■ ASSOCIATED CONTENT

Supporting Information

The Supporting Information is available free of charge on the ACS Publications website at DOI: 10.1021/acs.jpca.9b04406.

Two tables containing additional numerical results: computed vibrational corrections to the ground-state rotational constants of all title and selected test (PH_2, PD_2, PF_2, PH_3, PD_3) molecules as well as computed rotational g-tensors and related electronic contributions to the rotational constants of all title and closed-shell test (PH_3, PD_3) molecules (PDF)

■ AUTHOR INFORMATION

Corresponding Author

*E-mail: thiel@mpi-muelheim.mpg.de.

ORCID

Walter Thiel: 0000-0001-6780-0350

Notes

The authors declare no competing financial interest.

■ ACKNOWLEDGMENTS

This work was supported by the Max Planck Society.

■ REFERENCES

(1) Najib, H.; Ben Sari-Zizi, N.; Bürger, H.; Rahner, A.; Halonen, L. High-Resolution FTIR Investigation of PF_3 in the 300−550 cm^{-1} Region: The Ground, v_2 = 1, and v_4 = 1 States. *J. Mol. Spectrosc.* **1993**, *159*, 249−258.

(2) Ben Sari-Zizi, N.; Bürger, H.; Litz, M.; Najib, H.; Radtke, J. High Resolution FTIR Study of PF_3 in the 800−950 cm^{-1} Region. The ν_1 and ν_3 Fundamental and $\nu_2 + \nu_4$ Combination Bands. *J. Mol. Spectrosc.* **1996**, *177*, 46−57.

(3) Kisliuk, P.; Townes, C. H. The Microwave Spectra and Molecular Structure of Phosphorus and Arsenic Trichloride. *J. Chem. Phys.* **1950**, *18*, 1109−1111.

(4) Mirri, A. M.; Scappini, F.; Favero, P. G. Millimeter Wave Spectrum of PF_3 and PCl_3 and Force Constants Determination. *Spectrochim. Acta* **1965**, *21*, 965−971.

(5) Cazzoli, G. Force Constant Calculations of NCl_3 and PCl_3. *J. Mol. Spectrosc.* **1974**, *53*, 37−44.

(6) Carpenter, J. H.; Walters, A.; Rabbett, M. D.; Baker, J. G. The Orientation of the Electric Field Gradient Tensor in Gaseous PCl_3 by Millimeter-Wave and Supersonic-Jet Fourier Transform Microwave Spectroscopy. *J. Mol. Spectrosc.* **1988**, *131*, 77−88.

(7) Beckers, H.; Breidung, J.; Bürger, H.; Kuna, R.; Rahner, A.; Schneider, W.; Thiel, W. High-Resolution Rotation-Vibration Spectroscopy of Difluorophosphorane: A Combined Theoretical and Experimental Study. *J. Chem. Phys.* **1990**, *93*, 4603−4614.

(8) Beckers, H.; Bürger, H.; Rahner, A. FTIR Study of the ν_7 Band of PH_3F_2 near 340 cm^{-1}. *J. Mol. Spectrosc.* **1992**, *151*, 197−205.

(9) Takami, M.; Kuze, H. Cold Jet Infrared Absorption Spectroscopy: The ν_3 Band of PF_5. *J. Chem. Phys.* **1984**, *80*, 2314−2318.

(10) Dana, V.; Bordé, J.; Henry, L.; Valentin, A. Analysis of the Fourier Transform Spectrum of PF_5 around 946 cm^{-1}. *J. Mol. Spectrosc.* **1985**, *114*, 42−48.

(11) Prinz, H.; Kreiner, W. A. Resolution of the Q Branch in the ν_3 Fundamental of PF_5. *J. Mol. Spectrosc.* **1989**, *137*, 204−214.

(12) Styger, C.; Bauder, A. Pure Rotational Spectrum of Phosphorus Pentafluoride Observed by Microwave Fourier Transform Spectroscopy. *J. Mol. Spectrosc.* **1991**, *148*, 479−493. *J. Mol. Spectrosc.* **1992**, *151*, 536−536.

(13) Vázquez, J.; Stanton, J. F. Semiexperimental Equilibrium Structures: Computational Aspects. In *Equilibrium Molecular Structures*; Demaison, J., Boggs, J. E., Császár, A. G., Eds.; CRC Press: Boca Raton, FL, 2011; pp 53−87.

(14) Pulay, P.; Meyer, W.; Boggs, J. E. Cubic Force Constants and Equilibrium Geometry of Methane from Hartree−Fock and Correlated Wavefunctions. *J. Chem. Phys.* **1978**, *68*, 5077−5085.

(15) Pawłowski, F.; Jørgensen, P.; Olsen, J.; Hegelund, F.; Helgaker, T.; Gauss, J.; Bak, K. L.; Stanton, J. F. Molecular Equilibrium Structures from Experimental Rotational Constants and Calculated Vibration-Rotation Interaction Constants. *J. Chem. Phys.* **2002**, *116*, 6482−6496.

(16) Müller, H. S. P.; Maeda, A.; Thorwirth, S.; Lewen, F.; Schlemmer, S.; Medvedev, I. R.; Winnewisser, M.; De Lucia, F. C.; Herbst, E. Laboratory Spectroscopic Study of Isotopic Thioformaldehyde, H_2CS, and Determination of Its Equilibrium Structure. *Astron. Astrophys.* **2019**, *621*, A143.

DOI: 10.1021/acs.jpca.9b04406
J. Phys. Chem. A 2019, 123, 5600−5612

(17) Ruden, T. A.; Helgaker, T.; Jørgensen, P.; Olsen, J. Coupled-Cluster Connected Quadruples and Quintuples Corrections to the Harmonic Vibrational Frequencies and Equilibrium Bond Distances of HF, N_2, F_2, and CO. *J. Chem. Phys.* **2004**, *121*, 5874−5884.
(18) Heckert, M.; Kállay, M.; Gauss, J. Molecular Equilibrium Geometries Based on Coupled-Cluster Calculations Including Quadruple Excitations. *Mol. Phys.* **2005**, *103*, 2109−2115.
(19) Heckert, M.; Kállay, M.; Tew, D. P.; Klopper, W.; Gauss, J. Basis-Set Extrapolation Techniques for the Accurate Calculation of Molecular Equilibrium Geometries Using Coupled-Cluster Theory. *J. Chem. Phys.* **2006**, *125*, No. 044108.
(20) Puzzarini, C. Accurate Molecular Structures of Small- and Medium-Sized Molecules. *Int. J. Quantum Chem.* **2016**, *116*, 1513−1519.
(21) Breidung, J.; Thiel, W. Equilibrium Structures of Pyrazine, s-Triazine, and s-Tetrazine. *J. Phys. Chem. C* **2019**, *123*, 7940−7951.
(22) Werner, H.-J.; Adler, T. B.; Knizia, G.; Manby, F. R. Efficient Explicitly Correlated Coupled-Cluster Approximations. In *Recent Progress in Coupled Cluster Methods*; Čársky, P., Paldus, J., Pittner, J., Eds.; Springer: Dordrecht, 2010; pp 573−619.
(23) Hill, J. G.; Mazumder, S.; Peterson, K. A. Correlation Consistent Basis Sets for Molecular Core-Valence Effects with Explicitly Correlated Wave Functions: The Atoms B−Ne and Al−Ar. *J. Chem. Phys.* **2010**, *132*, No. 054108.
(24) Peterson, K. A.; Adler, T. B.; Werner, H.-J. Systematically Convergent Basis Sets for Explicitly Correlated Wavefunctions: The Atoms H, He, B−Ne, and Al−Ar. *J. Chem. Phys.* **2008**, *128*, No. 084102.
(25) Dréan, P.; Paplewski, M.; Demaison, J.; Breidung, J.; Thiel, W.; Beckers, H.; Bürger, H. Millimeter-Wave Spectra, *ab Initio* Calculations, and Structures of Fluorophosphane and Chlorophosphane. *Inorg. Chem.* **1996**, *35*, 7671−7678.
(26) Kurimura, H.; Yamamoto, S.; Egawa, T.; Kuchitsu, K. Geometrical Structure of PF_5 as Studied by Gas Electron Diffraction and Spectroscopic Data. *J. Mol. Struct.* **1986**, *140*, 79−86.
(27) Hansen, K. W.; Bartell, L. S. Electron Diffraction Study of the Structure of PF_5. *Inorg. Chem.* **1965**, *4*, 1775−1776.
(28) Spiridonov, V. P.; Ischenko, A. A.; Ivashkevich, L. S. A New Intensity Equation for Electron Diffraction Analysis: A Barrier to Pseudorotation in PF_5 from Diffraction Data. *J. Mol. Struct.* **1981**, *72*, 153−164.
(29) Macho, C.; Minkwitz, R.; Rohmann, J.; Steger, B.; Wölfel, V.; Oberhammer, H. The Chlorofluorophosphoranes PCl_nF_{5-n} (n = 1−4). Gas-Phase Structures and Vibrational Analyses. *Inorg. Chem.* **1986**, *25*, 2828−2835.
(30) McClelland, B. W.; Hedberg, L.; Hedberg, K. An Electron-Diffraction Investigation of the Molecular Structure and Thermal Dissociation of Gaseous PCl_5 at 90°C. *J. Mol. Struct.* **1983**, *99*, 309−313.
(31) Adams, W. J.; Bartell, L. S. Structure and Vibrational Assignments for PCl_5. An Electron Diffraction Study. *J. Mol. Struct.* **1971**, *8*, 23−30.
(32) Adler, T. B.; Knizia, G.; Werner, H.-J. A Simple and Efficient CCSD(T)-F12 Approximation. *J. Chem. Phys.* **2007**, *127*, 221106.
(33) Knizia, G.; Adler, T. B.; Werner, H.-J. Simplified CCSD(T)-F12 Methods: Theory and Benchmarks. *J. Chem. Phys.* **2009**, *130*, No. 054104.
(34) Purvis, G. D., III; Bartlett, R. J. A Full Coupled-Cluster Singles and Doubles Model: The Inclusion of Disconnected Triples. *J. Chem. Phys.* **1982**, *76*, 1910−1918.
(35) Hampel, C.; Peterson, K. A.; Werner, H.-J. A Comparison of the Efficiency and Accuracy of the Quadratic Configuration Interaction (QCISD), Coupled Cluster (CCSD), and Brueckner Coupled Cluster (BCCD) Methods. *Chem. Phys. Lett.* **1992**, *190*, 1−12.
(36) Raghavachari, K.; Trucks, G. W.; Pople, J. A.; Head-Gordon, M. A Fifth-Order Perturbation Comparison of Electron Correlation Theories. *Chem. Phys. Lett.* **1989**, *157*, 479−483.
(37) Knizia, G.; Werner, H.-J. Explicitly Correlated RMP2 for High-Spin Open-Shell Reference States. *J. Chem. Phys.* **2008**, *128*, 154103.
(38) Roothaan, C. C. J. Self-Consistent Field Theory for Open Shells of Electronic Systems. *Rev. Mod. Phys.* **1960**, *32*, 179−185.
(39) Watts, J. D.; Gauss, J.; Bartlett, R. J. Coupled-Cluster Methods with Noniterative Triple Excitations for Restricted Open-Shell Hartree−Fock and Other General Single Determinant Reference Functions. Energies and Analytical Gradients. *J. Chem. Phys.* **1993**, *98*, 8718−8733.
(40) Werner, H.-J.; Knowles, P. J.; Knizia, G.; Manby, F. R.; Schütz, M.; Celani, P.; Korona, T.; Lindh, R.; Mitrushenkov, A.; Rauhut, G.; et al. *MOLPRO*, version 2012.1, a Package of *ab Initio* Programs; 2012; see http://www.molpro.net.
(41) Werner, H.-J.; Knowles, P. J.; Knizia, G.; Manby, F. R.; Schütz, M. Molpro: A General-Purpose Quantum Chemistry Program Package. *WIREs Comput. Mol. Sci.* **2012**, *2*, 242−253.
(42) Noga, J.; Bartlett, R. J. The Full CCSDT Model for Molecular Electronic Structure. *J. Chem. Phys.* **1987**, *86*, 7041−7050. *J. Chem. Phys.* **1988**, *89*, 3401−3401.
(43) Scuseria, G. E.; Schaefer, H. F., III A New Implementation of the Full CCSDT Model for Molecular Electronic Structure. *Chem. Phys. Lett.* **1988**, *152*, 382−386.
(44) Stanton, J. F.; Gauss, J.; Watts, J. D.; Bartlett, R. J. A Direct Product Decomposition Approach for Symmetry Exploitation in Many-Body Methods. I. Energy Calculations. *J. Chem. Phys.* **1991**, *94*, 4334−4345.
(45) Dunning, T. H., Jr. Gaussian Basis Sets for Use in Correlated Molecular Calculations. I. The Atoms Boron through Neon and Hydrogen. *J. Chem. Phys.* **1989**, *90*, 1007−1023.
(46) Dunning, T. H., Jr.; Peterson, K. A.; Wilson, A. K. Gaussian Basis Sets for Use in Correlated Molecular Calculations. X. The Atoms Aluminum through Argon Revisited. *J. Chem. Phys.* **2001**, *114*, 9244−9253.
(47) Wilson, A. K.; van Mourik, T.; Dunning, T. H., Jr. Gaussian Basis Sets for Use in Correlated Molecular Calculations. VI. Sextuple Zeta Correlation Consistent Basis Sets for Boron through Neon. *J. Mol. Struct.: THEOCHEM* **1996**, *388*, 339−349.
(48) Watts, J. D.; Bartlett, R. J. The Coupled-Cluster Single, Double, and Triple Excitation Model for Open-Shell Single Reference Functions. *J. Chem. Phys.* **1990**, *93*, 6104−6105.
(49) Stanton, J. F.; Gauss, J.; Cheng, L.; Harding, M. E.; Matthews, D. A.; Szalay, P. G. with contributions from Auer, A. A.; Bartlett, R. J.; Benedikt, U.; Berger, C.; et al. *CFOUR, a Quantum Chemical Program Package*; For the current version, see http://www.cfour.de (accessed August 1, 2013).
(50) Bomble, Y. J.; Stanton, J. F.; Kállay, M.; Gauss, J. Coupled-Cluster Methods Including Noniterative Corrections for Quadruple Excitations. *J. Chem. Phys.* **2005**, *123*, No. 054101.
(51) Kállay, M.; Gauss, J. Approximate Treatment of Higher Excitations in Coupled-Cluster Theory. *J. Chem. Phys.* **2005**, *123*, 214105.
(52) Kállay, M.; Rolik, Z.; Ladjánszki, I.; Szegedy, L.; Ladóczki, B.; Csontos, J.; Kornis, B. *MRCC, a Quantum Chemical Program Suite*; 2013; see http://www.mrcc.hu.
(53) Kállay, M.; Surján, P. R. Higher Excitations in Coupled-Cluster Theory. *J. Chem. Phys.* **2001**, *115*, 2945−2954.
(54) Gauss, J.; Stanton, J. F. Analytic Gradients for the Coupled-Cluster Singles, Doubles, and Triples (CCSDT) Model. *J. Chem. Phys.* **2002**, *116*, 1773−1782.
(55) Kucharski, S. A.; Bartlett, R. J. Recursive Intermediate Factorization and Complete Computational Linearization of the Coupled-Cluster Single, Double, Triple, and Quadruple Excitation Equations. *Theor. Chim. Acta* **1991**, *80*, 387−405.
(56) Kucharski, S. A.; Bartlett, R. J. The Coupled-Cluster Single, Double, Triple, and Quadruple Excitation Method. *J. Chem. Phys.* **1992**, *97*, 4282−4288.
(57) Oliphant, N.; Adamowicz, L. Coupled-Cluster Method Truncated at Quadruples. *J. Chem. Phys.* **1991**, *95*, 6645−6651.

DOI: 10.1021/acs.jpca.9b04406
J. Phys. Chem. A 2019, 123, 5600−5612

(58) Pople, J. A.; Nesbet, R. K. Self-Consistent Orbitals for Radicals. *J. Chem. Phys.* **1954**, *22*, 571−572.
(59) Wolf, A.; Reiher, M.; Hess, B. A. The Generalized Douglas-Kroll Transformation. *J. Chem. Phys.* **2002**, *117*, 9215−9226.
(60) Reiher, M.; Wolf, A. Exact Decoupling of the Dirac Hamiltonian. I. General Theory. *J. Chem. Phys.* **2004**, *121*, 2037−2047.
(61) Reiher, M.; Wolf, A. Exact Decoupling of the Dirac Hamiltonian. II. The Generalized Douglas-Kroll-Hess Transformation up to Arbitrary Order. *J. Chem. Phys.* **2004**, *121*, 10945−10956.
(62) Peterson, K. A.; Dunning, T. H., Jr. Accurate Correlation Consistent Basis Sets for Molecular Core-Valence Correlation Effects: The Second Row Atoms Al−Ar, and the First Row Atoms B−Ne Revisited. *J. Chem. Phys.* **2002**, *117*, 10548−10560.
(63) Kendall, R. A.; Dunning, T. H., Jr.; Harrison, R. J. Electron Affinities of the First-Row Atoms Revisited. Systematic Basis Sets and Wave Functions. *J. Chem. Phys.* **1992**, *96*, 6796−6806.
(64) Woon, D. E.; Dunning, T. H., Jr. Gaussian Basis Sets for Use in Correlated Molecular Calculations. III. The Atoms Aluminum through Argon. *J. Chem. Phys.* **1993**, *98*, 1358−1371.
(65) De Jong, W. A.; Harrison, R. J.; Dixon, D. A. Parallel Douglas-Kroll Energy and Gradients in NWChem: Estimating Scalar Relativistic Effects Using Douglas-Kroll Contracted Basis Sets. *J. Chem. Phys.* **2001**, *114*, 48−53.
(66) Knowles, P. J.; Hampel, C.; Werner, H.-J. Coupled Cluster Theory for High Spin, Open Shell Reference Wave Functions. *J. Chem. Phys.* **1993**, *99*, 5219−5227. *J. Chem. Phys.* **2000**, *112*, 3106−3107.
(67) Margulès, L.; Herbst, E.; Ahrens, V.; Lewen, F.; Winnewisser, G.; Müller, H. S. P. The Phosphidogen Radical, PH_2: Terahertz Spectrum and Detectability in Space. *J. Mol. Spectrosc.* **2002**, *211*, 211−220.
(68) Hirao, T.; Hayakashi, S.; Yamamoto, S.; Saito, S. Microwave Spectrum of the PD_2 Radical in the $^2B_1$ Ground Electronic State. *J. Mol. Spectrosc.* **1998**, *187*, 153−162.
(69) Saito, S.; Endo, Y.; Hirota, E. The Microwave Spectrum of the PF_2 Radical in the $X\ ^2B_1$ Ground Vibronic State. *J. Chem. Phys.* **1986**, *85*, 1778−1784.
(70) Fusina, L.; Di Lonardo, G. The ν_2 and ν_4 Bending Fundamentals of Phosphine (PH_3). *J. Mol. Struct.* **2000**, *517*−*518*, 67−78.
(71) Canè, E.; Fusina, L.; Bürger, H.; Jerzembeck, W.; Brünken, S.; Lewen, F.; Winnewisser, G. The Ground State Spectroscopic Parameters and Equilibrium Structure of PD_3. *J. Mol. Spectrosc.* **2002**, *215*, 1−9.
(72) Ceausu-Velcescu, A.; Pracna, P.; Breidung, J.; Thiel, W.; Badaoui, M. The $\nu_4 = 1$ and $\nu_4 = 2$ Rovibrational Levels of PF_3 Revisited: New Solutions for Old Topics. *J. Mol. Spectrosc.* **2015**, *316*, 11−21.
(73) Mills, I. M. Vibration-Rotation Structure in Asymmetric- and Symmetric-Top Molecules. In *Molecular Spectroscopy: Modern Research*; Rao, K. N., Mathews, C. W., Eds.; Academic Press: New York, 1972; pp 115−140.
(74) Puzzarini, C.; Heckert, M.; Gauss, J. The Accuracy of Rotational Constants Predicted by High-Level Quantum-Chemical Calculations. I. Molecules Containing First-Row Atoms. *J. Chem. Phys.* **2008**, *128*, 194108.
(75) Schneider, W.; Thiel, W. Anharmonic Force Fields from Analytic Second Derivatives: Method and Application to Methyl Bromide. *Chem. Phys. Lett.* **1989**, *157*, 367−373.
(76) Gauss, J.; Stanton, J. F. Analytic CCSD(T) Second Derivatives. *Chem. Phys. Lett.* **1997**, *276*, 70−77.
(77) Szalay, P. G.; Gauss, J.; Stanton, J. F. Analytic UHF-CCSD(T) Second Derivatives: Implementation and Application to the Calculation of the Vibration-Rotation Interaction Constants of NCO and NCS. *Theor. Chem. Acc.* **1998**, *100*, 5−11.
(78) Perrin, A.; Demaison, J.; Flaud, J.-M.; Lafferty, W. J.; Sarka, K. Spectroscopy of Polyatomic Molecules: Determination of the Rotational Constants. In *Equilibrium Molecular Structures*; Demaison, J., Boggs, J. E., Császár, A. G., Eds.; CRC Press: Boca Raton, FL, 2011; pp 89−124.
(79) Gauss, J.; Ruud, K.; Helgaker, T. Perturbation-Dependent Atomic Orbitals for the Calculation of Spin-Rotation Constants and Rotational *g* Tensors. *J. Chem. Phys.* **1996**, *105*, 2804−2812.
(80) Gauss, J.; Ruud, K.; Kállay, M. Gauge-Origin Independent Calculation of Magnetizabilities and Rotational *g* Tensors at the Coupled-Cluster Level. *J. Chem. Phys.* **2007**, *127*, No. 074101.
(81) Kukolich, S. G.; Flygare, W. H. The Molecular Zeeman Effect in PH_2D and PHD_2 and the Molecular *g*-Values, Magnetic Susceptibilities, and Molecular Quadrupole Moment in PH_3. *Chem. Phys. Lett.* **1970**, *7*, 43−46.
(82) Hüttner, W.; Nowicki, P.; Gamperling, M. Rotational Magnetism in the Ground and $(000°1^1)$ Vibrational States of Trifluorophosphine, PF_3. *Chem. Phys. Lett.* **1998**, *288*, 553−560.
(83) Feller, D. The Role of Databases in Support of Computational Chemistry Calculations. *J. Comput. Chem.* **1996**, *17*, 1571−1586.
(84) Schuchardt, K. L.; Didier, B. T.; Elsethagen, T.; Sun, L.; Gurumoorthi, V.; Chase, J.; Li, J.; Windus, T. L. Basis Set Exchange: A Community Database for Computational Sciences. *J. Chem. Inf. Model.* **2007**, *47*, 1045−1052.
(85) Michauk, C.; Gauss, J. Perturbative Treatment of Scalar-Relativistic Effects in Coupled-Cluster Calculations of Equilibrium Geometries and Harmonic Vibrational Frequencies Using Analytic Second-Derivative Techniques. *J. Chem. Phys.* **2007**, *127*, No. 044106.
(86) Hughes, R. A.; Brown, J. M. A Determination of the Vibrational Anharmonicity of PD in Its $X\ ^3\Sigma^-$ State. *J. Mol. Spectrosc.* **1997**, *185*, 197−201.
(87) Ram, R. S.; Bernath, P. F. Fourier Transform Infrared Emission Spectroscopy of ND and PH. *J. Mol. Spectrosc.* **1996**, *176*, 329−336.
(88) Ohashi, N.; Kawaguchi, K.; Hirota, E. Far-Infrared Laser Magnetic Resonance Spectra of the PH and PD Radicals in $X\ ^3\Sigma^-$. *J. Mol. Spectrosc.* **1984**, *103*, 337−349.
(89) Yamada, C.; Chang, M. C.; Hirota, E. Infrared Diode Laser Spectroscopy of the PF Radical. *J. Chem. Phys.* **1987**, *86*, 3804−3806.
(90) Douglas, A. E.; Frackowiak, M. The Electronic Spectra of PF and PF^+. *Can. J. Phys.* **1962**, *40*, 832−849.
(91) Kanamori, H.; Yamada, C.; Butler, J. E.; Kawaguchi, K.; Hirota, E. Infrared Diode Laser Spectroscopy of the PCl Radical. *J. Chem. Phys.* **1985**, *83*, 4945−4948.
(92) Puzzarini, C.; Barone, V. Toward Spectroscopic Accuracy for Open-Shell Systems: Molecular Structure and Hyperfine Coupling Constants of H_2CN, H_2CP, NH_2, and PH_2 as Test Cases. *J. Chem. Phys.* **2010**, *133*, 184301.
(93) Coriani, S.; Marchesan, D.; Gauss, J.; Hättig, C.; Helgaker, T.; Jørgensen, P. The Accuracy of *ab Initio* Molecular Geometries for Systems Containing Second-Row Atoms. *J. Chem. Phys.* **2005**, *123*, 184107.
(94) Kawashima, Y.; Cox, A. P. Microwave l-Type Resonance Transitions of the $\nu_4 = 1$ State in PF_3: Detailed Interactions and Molecular Structure. *J. Mol. Spectrosc.* **1977**, *65*, 319−329.
(95) Graner, G.; Hirota, E.; Iijima, T.; Kuchitsu, K.; Ramsay, D. A.; Vogt, J.; Vogt, N. In *Structure Data of Free Polyatomic Molecules*; Landolt-Börnstein, Numerical Data and Functional Relationships in Science and Technology (New Series), Vol. *II/25A*; Kuchitsu, K., Ed.; Springer: Berlin, 1998.
(96) Hedberg, K.; Iwasaki, M. Effect of Temperature on the Structure of Gaseous Molecules. Molecular Structure of PCl_3 at 300° and 505 K. *J. Chem. Phys.* **1962**, *36*, 589−594.
(97) Kisiel, Z. Least-Squares Mass-Dependence Molecular Structures for Selected Weakly Bound Intermolecular Clusters. *J. Mol. Spectrosc.* **2003**, *218*, 58−67.
(98) Muetterties, E. L.; Mahler, W.; Schmutzler, R. Stereochemistry of Phosphorus(V) Fluorides. *Inorg. Chem.* **1963**, *2*, 613−618.
(99) Muetterties, E. L.; Mahler, W.; Packer, K. J.; Schmutzler, R. Five-Coordinate Stereochemistry. *Inorg. Chem.* **1964**, *3*, 1298−1303.
(100) Musher, J. I. The Chemistry of Hypervalent Molecules. *Angew. Chem., Int. Ed. Engl.* **1969**, *8*, 54−68.

DOI: 10.1021/acs.jpca.9b04406
J. Phys. Chem. A 2019, 123, 5600−5612

(101) Woon, D. E.; Dunning, T. H., Jr. Theory of Hypervalency: Recoupled Pair Bonding in SF_n (n = 1−6). *J. Phys. Chem. A* **2009**, *113*, 7915−7926.
(102) Woon, D. E.; Dunning, T. H., Jr. Recoupled Pair Bonding in PF_n (n = 1−5). *J. Phys. Chem. A* **2010**, *114*, 8845−8851.
(103) Berry, R. S. Correlation of Rates of Intramolecular Tunneling Processes, with Application to Some Group V Compounds. *J. Chem. Phys.* **1960**, *32*, 933−938.

DOI: 10.1021/acs.jpca.9b04406
J. Phys. Chem. A 2019, 123, 5600−5612